

Cite this: *Polym. Chem.*, 2017, **8**, 5071

# Improving tumor chemotherapy effect using an injectable self-healing hydrogel as drug carrier†

Lei Yang,<sup>‡a</sup> Yongsan Li,<sup>‡b,c</sup> Yanzi Gou,<sup>d</sup> Xing Wang,<sup>\*c</sup> Xinming Zhao<sup>\*a</sup> and Lei Tao<sup>ID \*b</sup>

Chemotherapy has contributed greatly in clinical anti-tumor treatment. However, the traditional method of drug delivery by intravenous injection has several drawbacks, such as low delivery efficiency, high toxicity and frequent pain caused by injection. To overcome these defects, intra-tumor injection has been proposed in recent years, and the development of suitable carriers to locate the drug at the desired position for optimum dispersal is crucial to realize the superiority of intra-tumor injection. Herein, we report the application of a chitosan-based self-healing hydrogel, constructed through Schiff's bases, as an injectable drug carrier for *in vivo* intra-tumor therapy. This smart carrier could deliver highly concentrated anti-tumor drug (Taxol) to the desired position (human hepatocarcinoma tumor) for steady *in situ* release at a safe level. The self-healing drug carrier could adapt to the intra-tumor structure and regenerate as a whole, thus avoiding the fast leak of loaded drug, leading to admirable therapeutic effects compared with controls (direct injection of drug solution or use of non-self-healable thermal-sensitive hydrogel as the drug carrier). Due to its excellent biocompatibility and high operability, this injectable self-healing hydrogel might be a promising drug carrier for tumor chemotherapy and other medical applications.

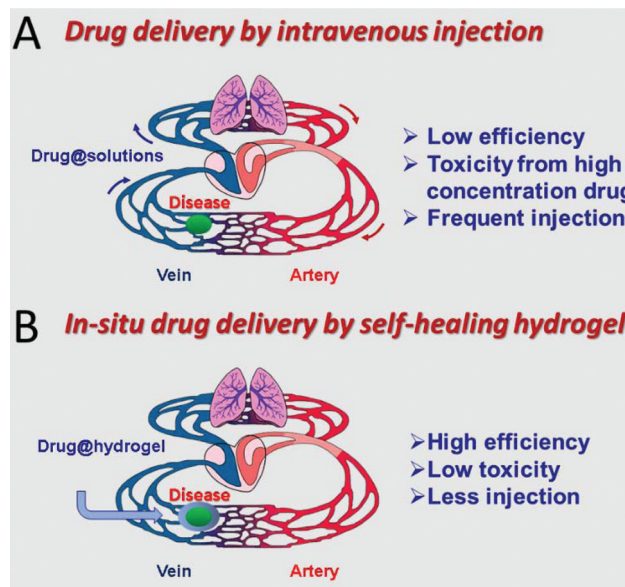
Received 19th January 2017,  
Accepted 6th March 2017

DOI: 10.1039/c7py00112f

rs.c.li/polymers

## 1. Introduction

Efficient delivery of a drug to the disease position is crucial to realize the therapeutic effect of the drug.<sup>1–3</sup> Traditionally, drugs can be administered through intravenous or subcutaneous injections;<sup>4,5</sup> the drug has to travel a long way in the circulation system to reach the disease position, and the drug concentration is severely diluted due to blood or body fluid. As a result, most of the drug will be lost during circulation. To maintain enough drug concentration at the disease position, frequent administration is normally necessary, resulting in pain to the patients<sup>6,7</sup> (Scheme 1A). Therefore, numerous strategies based on passive targeting (EPR effect) or active targeting



**Scheme 1** Schematic of the difference between (A) traditional drug delivery by intravenous cycling and (B) *in situ* drug delivery by self-healing hydrogel.

<sup>a</sup>Department of Diagnostic Radiology, National Cancer Center/Cancer Hospital, Chinese Academy of Medical Science and Peking Union Medical College, Beijing 100021, P. R. China. E-mail: xinmingzh@sina.com

<sup>b</sup>The Key Laboratory of Bioorganic Phosphorus Chemistry & Chemical Biology (Ministry of Education), Department of Chemistry, Tsinghua University, Beijing 100084, P. R. China. E-mail: leitao@mail.tsinghua.edu.cn

<sup>c</sup>Beijing Laboratory of Biomedical Materials, Beijing University of Chemical Technology, Beijing 100029, P. R. China. E-mail: wangxing@mail.buct.edu.cn

<sup>d</sup>Science and Technology on Advanced Ceramic Fibers and Composites Laboratory, National University of Defense Technology, 137, Yanwachi Street, Changsha, Hunan, 410073, P. R. China

† Electronic supplementary information (ESI) available: Details of *in vivo* experiments, hydrogel analyses etc. See DOI: 10.1039/c7py00112f

‡ These authors contributed equally to this work.

(bio-targeting molecule modification) have been designed to enrich the drugs at desired positions after injection,<sup>8–13</sup> and several promising results have been achieved in cell and

animal experiments.<sup>14–19</sup> However, due to the huge difference between human and animals with respect to their circulatory and metabolic systems, few of the abovementioned methods can finally cross the huge gap between bench and bed to enter clinic trials,<sup>20</sup> implying that a drug delivery strategy that avoids the involvement of the circulatory system might be the key to develop applicable drug-delivery approaches.

Self-healing hydrogel is a smart, soft material,<sup>21,22</sup> the damage of which can trigger an auto-repair process to regenerate an integral hydrogel. Due to this unique capability, self-healing hydrogels are considered as promising drug carriers.<sup>23,24</sup> After injecting a drug-contained self-healing hydrogel to the affected area, the hydrogel can heal itself under physiological condition, avoiding the long journey in circulation system, and be directly located at the desired position in high-concentrations, leading to improved utilization efficiency and decreased toxicity to normal tissues<sup>25,26</sup> (Scheme 1B).

Nowadays, some self-healing hydrogels have been developed and used as injectable drug carriers,<sup>27–29</sup> opening a new door to efficient delivery of drugs. However, most of these self-healing hydrogels were prepared using expensive and complex gelators,<sup>30–32</sup> limiting their large-scale preparation and subsequent clinical application. Recently, our group developed a biocompatible self-healing hydrogel using chitosan derivatives and synthetic difunctional polyethylene glycol (DF-PEG).<sup>33–36</sup> The amino groups on glycol-chitosan were crosslinked by the benzaldehyde group at the PEG chain ends to form a Schiff base, which is a well-known dynamic chemical linkage in aqueous solutions, resulting in a chitosan-PEG (CP) hydrogel constructed by a dynamic network. In our previous research, the excellent self-healing ability and biocompatibility of the CP hydrogels have been verified. In the current research, CP hydrogel was employed as a drug-carrier to deliver anti-tumor drugs through intra-tumor injection to verify the advantage of self-healing hydrogel as a drug carrier.

## 2. Experimental

### 2.1. Materials

DF-PEG ( $M_n \sim 4000 \text{ g mol}^{-1}$ ) was synthesized following a procedure mentioned in our previous study<sup>33</sup> and analyzed in detail (Fig. S1 and S2†). Glycol chitosan (Wako Pure Chemical Industries, 90% degree of deacetylation), Pluronic F127 (Sinopharm Chemical Reagent), Taxol (Beijing Union Pharm), Taxol (Dalian Meilun Biological Technology. Co. Ltd), 4-carboxybenzaldehyde (Aladdin, 99%), *N,N'*-dicyclohexylcarbodiimide (DCC, Aladdin, 99%), 4-dimethylaminoipyridine (DMAP, Aladdin, 99%) and PEG (Sinopharm Chemical Reagent,  $M_w$  4000) were used as purchased. All solvents were purchased from Sinopharm Chemical Reagent and used directly without further purification. Female nude mice (Balb/c-Nu) were ordered from Charles River. Human hepatocarcinoma tumor (BEL-7402) was acquired from National Cancer Center/Cancer Hospital.

### 2.2. Preparation of the hydrogels

DF-PEG solution was prepared by dissolving DF-PEG (0.11 g) in a saline solution (0.9% NaCl, 800  $\mu\text{L}$ ). The chitosan solution was prepared by dissolving glycol-chitosan (0.033 g) in a saline solution (0.9% NaCl, 1000  $\mu\text{L}$ ). The Taxol-containing chitosan hydrogel was prepared as follows: Taxol ethanol solution (200  $\mu\text{L}$ , 20  $\text{mg mL}^{-1}$ ) was first added into chitosan solution (1000  $\mu\text{L}$ ), followed by triturating 15–20 times to evenly distribute the drug. Then, DF-PEG solution (800  $\mu\text{L}$ ) was added to generate a transparent Taxol-containing hydrogel for drug delivery.

As a control, a Taxol-containing Pluronic F127 hydrogel, a traditional thermal-sensitive hydrogel, was also prepared by the following method: Pluronic F127 (0.37 g) was dissolved in 1800  $\mu\text{L}$  of saline solution (0.9% NaCl) and subsequently mixed with Taxol ethanol solution (200  $\mu\text{L}$ , 20  $\text{mg mL}^{-1}$ ). The sol-gel transformation was tested to occur when the temperature reaches 35  $^\circ\text{C}$ .

### 2.3. Rheology analysis of the gelation process

The rheology analyses of the hydrogel were carried out to evaluate the mechanical strength of the CP hydrogel. Typically, glycol chitosan solution (0.2 g, 3%) was spread on the parallel plate of the rheometer. Then, DF-PEG aqueous solution (0.2 g, 2%) was evenly added dropwise onto the chitosan solution surface and quickly mixed using a pipette. The storage modulus ( $G'$ ) and loss modulus ( $G''$ ) versus frequency analyses were carried out using a steel plate (diameter: 20 mm) and performed at 1% strain and 6.3  $\text{rad s}^{-1}$ .

### 2.4. Qualitative self-healing experiment

To evaluate the self-healing ability of the CP hydrogel, an injection experiment was performed. As shown in Fig. 1, the CP hydrogel was prepared in a syringe by mixing the glycol-chitosan solution and the DF-PEG solution, (blue dye was added for easy observation). Then, the hydrogel was injected into a vial with 0.9% saline solution and kept at 37  $^\circ\text{C}$ . A thermo-sensitive injectable Pluronic F127 hydrogel (red dye added for easy observation) was used as a control.

### 2.5. Quantitative self-healing experiment

A piece of CP hydrogel (400  $\mu\text{L}$ ) was first prepared on the parallel plate as a routine. After complete gelation of the hydrogel, it was cut into 25 pieces to mimic the injection yet maintain the contacting area between the hydrogel and the upper steel plate. Analysis was performed to monitor the self-healing process of the broken hydrogels. After the mechanical strength of the self-healed hydrogel plateaued in time-dependent mode, a frequency-dependent rheological test was carried out to evaluate the storage modulus ( $G'$ ) as well as the loss modulus ( $G''$ ) of the self-healed hydrogel.

### 2.6. Cumulative release of Taxol

A 7-day cumulative release of Taxol from the CP hydrogel was studied using a UV-vis spectrometer (230 nm). A Taxol-laden

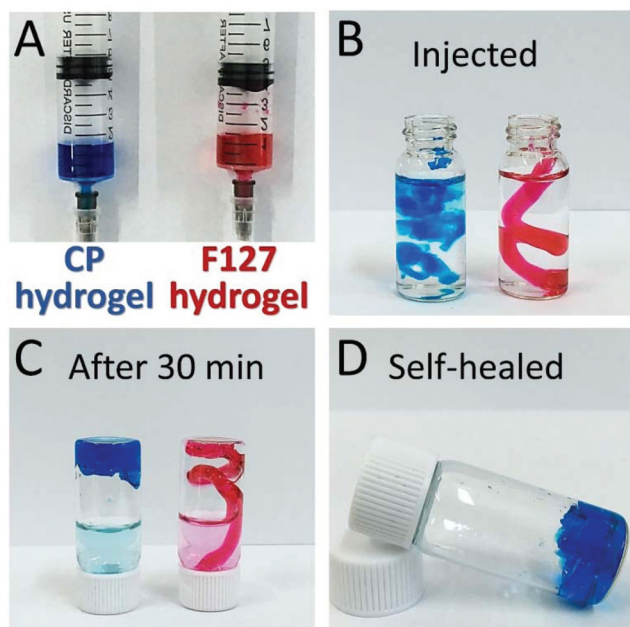


**Fig. 1** Pictures of the CP hydrogel (blue) and Pluronic F127 hydrogel (red) (A) loaded in syringes, (B) just injected and (C) after 30 minutes; (D) the self-healed CP hydrogel.

hydrogel (1.0 mL) was prepared in a centrifuge tube and saline solution (1.0 mL) was added as the release media, as shown in Fig. 3A and A1. The release system was kept in a 37 °C incubator to mimic the *in vivo* release environment. Sample solutions (1.0 mL) were taken out at designated time points to analyze the release amount of Taxol, while the same volume of saline solution was replaced in the centrifuge tubes for successive release. The signal of the Taxol solution (200  $\mu$ L Taxol ethanol solution with 800  $\mu$ L saline water) was defined as 100%. The release of Taxol from a Pluronic F127 hydrogel (TAX-F127) was studied as the control.

### 2.7. *In vivo* tests

All *in vivo* tests were performed under the technical guidelines for non-clinical study of cytotoxic anti-tumor drugs issued by CFDA and authorized by the ethics committee of Cancer Hospital, Chinese Academy of Medical Science. Human hepatocarcinoma tumor (BEL-7402) was first implanted into the right femur of 24 female nude mice (Balb/c-Nu). After the tumors grew to about 100 mm<sup>3</sup>, the nude mice were divided into 4 groups and treated separately. The solutions were sterilized by passing through 0.22 micron bacteria-retentive filters. Then, 50  $\mu$ L of sterilized Taxol-loaded CP hydrogel (TAX-CP) was prepared and injected into the tumor after anaesthetizing the mice with pentobarbital. The weight of the mice and the size of tumors were recorded at different time points. All mice were sacrificed on the 18<sup>th</sup> day and the solid tumors were dissected. The tumor growth inhibition (TGI%) was calculated based on the tumor mass,<sup>37</sup> taking the blank group as 0%. Histology images of tumor slices from the mice (with H&E

staining) were subsequently acquired using an optical microscope. As controls, Pluronic Taxol-loaded F127 hydrogel (TAX-F127), Taxol solution (TAX-H<sub>2</sub>O) and saline water (blank) were used following the same procedure.

## 3. Results and discussion

### 3.1. Qualitative self-healing experiment

A preliminary injection experiment was performed to estimate the self-healing property of the CP hydrogel qualitatively. The CP hydrogel and Pluronic F127 hydrogel were prepared in two syringes with different colors (Fig. 1A), injected into the saline solution (Fig. 1B) and kept in a 37 °C incubator to mimic the *in vivo* condition. The broken CP hydrogel pieces generally self-healed to reform an entire piece of gel within 30 min. On the contrary, the Pluronic F127 hydrogel retained the shape as it was when injected (Fig. 1C), highlighting the remarkable self-healing ability of the CP hydrogel.

### 3.2. Quantitative self-healing experiment

Prior to the quantitative analysis of the self-healing capability of the CP hydrogel, a set of typical rheology tests were carried out to monitor the gelation process and the mechanical strength of the original CP hydrogel (without injection). As shown in Fig. 2A, the storage modulus ( $G'$ ) surpassed the loss modulus ( $G''$ ) in 2 min, demonstrating the rapid crosslinking process. The storage modulus continued increasing to reach the maximum ( $\sim$ 4000 Pa) in around 20 min (Fig. 2A and B). Based on these results, modified rheology tests were performed to follow the self-healing process by monitoring the modulus of the self-healed hydrogel. First, a CP hydrogel was prepared on the parallel plate of the rheometer and kept for

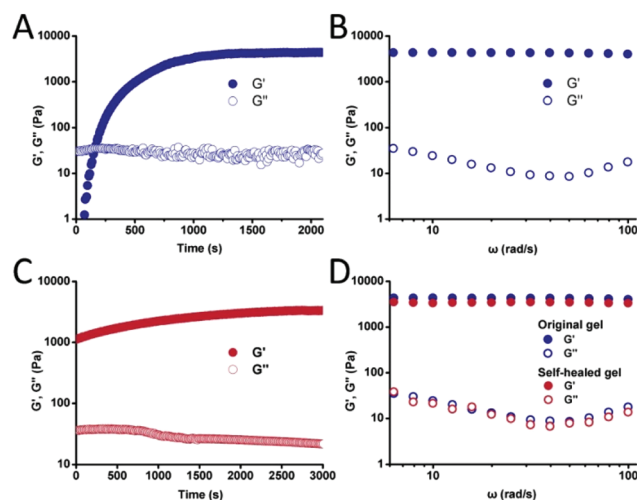


**Fig. 2** Rheology analyses of (A) the gelation process; (B) storage modulus  $G'$  (solid) and loss modulus  $G''$  (hollow) of the CP hydrogel; (C) the self-healing process; (D) storage modulus  $G'$  (solid) and loss modulus  $G''$  (hollow) of the original (red) and self-healed (blue) CP hydrogel. Sweeps were performed at 1% strain and 6.3 rad s<sup>-1</sup> in A, C; 1% strain in B, D.

30 min until the storage modulus stabilized around the maximum value ( $\sim 4000$  Pa, Fig. 2D, blue points). Then, the CP hydrogel was cut into pieces to mimic the damage process caused by injection while maintaining the contact surface between the broken hydrogel and the upper measuring steel plate. Then, the storage modulus *versus* time was recorded to monitor the restoring strength of the hydrogel. As shown in Fig. 2C, the storage modulus was found to drop to around 1000 Pa after the cutting and recovered with time to finally reach a similar level as the original hydrogel ( $\sim 3800$  Pa, Fig. 2D, red points), indicating the excellent self-healing ability of the CP hydrogel quantitatively. Moreover, the shear-thin data was also recorded by the rheometer (Fig. S3<sup>†</sup>), confirming the self-healing ability of the hydrogel.

### 3.3. Cumulative release of Taxol

As a drug carrier, an *in vitro* 7-day cumulative release of Taxol from the CP hydrogel was detected using a UV-Vis spectrometer at 230 nm. Briefly, the Taxol-loaded hydrogels were prepared and immersed in saline solution (Fig. 3A and A1) and kept at 37 °C. The cumulative release profile of the released Taxol is shown in Fig. 3B (blue points). With an initial 2-day high release period, 33% of Taxol was released from the CP hydrogel, followed by a slow release in the remainder of the testing process to reach a cumulative release of around 50% in 7 days. As a control, the release behavior of Taxol from a Pluronic F127 hydrogel was also studied with the same process (Fig. 3B, orange points). Moreover, 53% of Taxol was detected in the first 2 days with a rather slow continuing release to reach a total cumulative release of around 64% after 7 days. The difference in cumulative release between two hydrogels might lie in the inner structure of the two hydrogels. Differing from the Pluronic F127 hydrogel constructed through physical crosslinking, the CP hydrogel has a highly crosslinked network constructed by chemical Schiff base linkages, providing better location of the drug within the crosslinked network and avoiding the explosive release of the drug and unwanted adverse outcomes.

### 3.4. *In vivo* tests

Taxol-containing CP hydrogel was subsequently applied to the *in vivo* intra-tumor injection experiment to evaluate the

improved therapeutic effect by the drug carrier to the contained drug. For parallel control, a blank group (50  $\mu$ L of saline water), a positive group (50  $\mu$ L of Taxol solution) as well as a hydrogel control group TAX-F127 (50  $\mu$ L, Taxol in Pluronic F127 hydrogel) were also used for the intra-tumor injection by the same method.

A series of images of the tumor-bearing mice were taken after the 18-day tumor therapy (Fig. 4B). It is clearly seen that the tumor almost disappeared after treating the mice with TAX-CP, whilst the tumors in control groups had different degrees of growth compared with that before the treatment, illustrating the excellent therapy effect in using the self-healing hydrogel as the drug carrier. The tumor volumes of each test group throughout the entire observation process were also recorded (Fig. 4C). The tumor grew rapidly in the blank group, indicating that the established solid tumor model could keep growing like its clinical counterpart. After injecting TAX-H<sub>2</sub>O, the growth of solid tumors was suppressed compared with the blank group, demonstrating the distinct anti-tumor efficacy of TAX. The TAX in F127 group also achieved a similar therapeutic outcome as the TAX-H<sub>2</sub>O group,

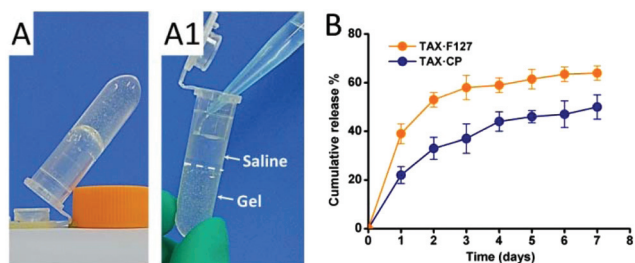


Fig. 3 (A) Taxol-containing CP hydrogel for cumulative release test. (A1) Adding saline, the release media, on the top of hydrogel. (B) The Taxol release profile of the CP hydrogel and the Pluronic F127 hydrogel.

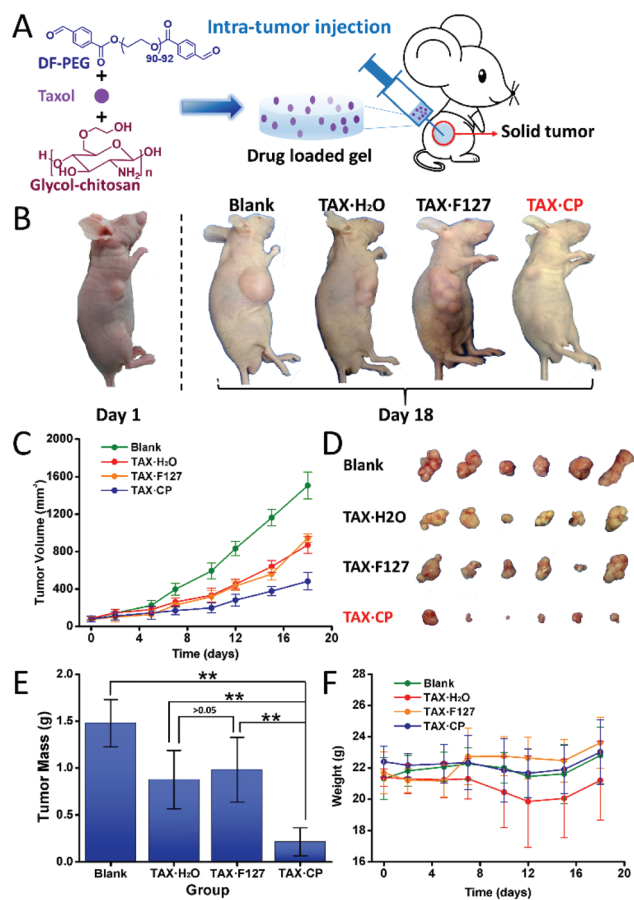


Fig. 4 (A) Schematic of the intra-tumor injection experiment. (B) Pictures of nude mice from different groups. (C) The tumor volume of mice in four groups. (D) The picture of the dissected tumors of the four groups on the 18<sup>th</sup> day. (E) The mass of the dissected tumors on the 18<sup>th</sup> day. (F) Weight changes of mice during the observation period.

indicating that F127 hydrogel did not improve the therapy efficacy. However, in the TAX-CP group, the tumor volumes were significantly decreased after the injection of Taxol with assistance of the CP hydrogel, suggesting that CP hydrogel could not only deliver Taxol to the tumor but could also promote the anti-tumor effect of the loaded chemo-drugs.

Subsequently, all mice were sacrificed after 18 days of therapy and the dissected tumors were imaged (Fig. 4D), which showed good accordance with the observed results, as shown in Fig. 4B. The tumors of the blank group (saline water) had the biggest volume (Fig. 4D). Tumors from the TAX-H<sub>2</sub>O group appeared smaller than the blank group, demonstrating the efficacy of the injected free drug. Tumors of the TAX-F127 group were around the same size as those of the TAX-H<sub>2</sub>O group, suggesting that F127 might not be a better drug carrier for intra-tumor injection. The tumors of the TAX-CP group were the smallest among the 4 groups, illustrating the advancement of the CP hydrogel as a drug carrier to improve the therapeutic effect of the anti-tumor drug.

Tumor growth inhibition (TGI) values, based on the tumors' masses, were calculated to quantitatively evaluate the therapeutic effect (Fig. 4E). With a TGI of 85%, the CP hydrogel exhibited the best anti-tumor effect, which was much higher than the free Taxol group (TGI ~41%) and the F127 group (TGI ~34%). The statistical analyses also suggested that the group treated by the CP hydrogel possesses significant differences from any other group ( $P < 0.01$ ). On the other hand, no significant difference between the Pluronic F127 group and the free Taxol group was observed, confirming that the self-healing CP hydrogel is a superior candidate than Pluronic F127 hydrogel as a drug carrier, particularly in intra-tumor injection usage.

The different performance of these two hydrogels might be related to the following reasons: (1) different from F127 hydrogel, which is simply constructed through physical crosslinking, the CP hydrogel is crosslinked by Schiff base linkages, which might provide more stable release of loaded drug from the network; (2) the unique self-healing ability of the CP hydrogel enables it to rebuild as a whole after injection to avoid the leak of the embedded Taxol, leading to long-term anti-tumor efficiency.

Toxicity of the therapy is also vital in chemotherapy. The variation in the weights of the nude mice at different time points was also recorded, as shown in Fig. 4F. The average weight of the blank group (saline water) was marked as a reference. The weight of the TAX-H<sub>2</sub>O group was the lowest, which might be due to the high toxicity of naked TAX. Moreover, the weights of both TAX-F127 and TAX-CP groups kept steady, even with a slight rise during the entire observation process, suggesting that both hydrogels could successfully reduce the toxicity of naked TAX to control the release of drugs at a safe level.

Combined with the abovementioned anti-tumor measurements, the CP hydrogel demonstrated more advantages than traditional treatments (direct injection or using traditional hydrogel as the drug carrier) by reducing drug toxicity and enhancing drug efficacy.

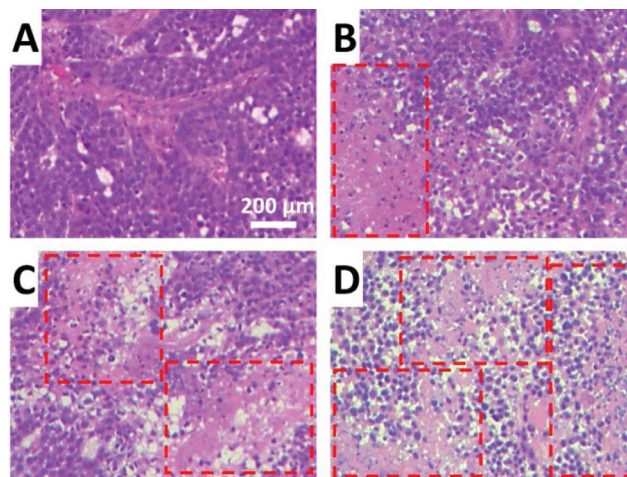


Fig. 5 H&E staining of the tumor slices from different groups: (A) blank; (B) TAX-H<sub>2</sub>O; (C) TAX-F127; (D) TAX-CP. Necrosis of cells is marked by red squares.

### 3.5. Histology images of tumor slices

To study the therapeutic difference among the four different treated groups at the tissue level, tumor slices with H&E histological staining were also analyzed (Fig. 5). No remaining hydrogel was noticed in the slices (Fig. 5C and D), indicating good biodegradability of the applied hydrogels. Fig. 5A shows the cells in the blank group that exhibited normal morphology, suggesting that tumors could tolerate the saline water well, while in Fig. 5B, for the TAX-H<sub>2</sub>O group, evident tumor cell necrosis as well as nuclear cleavage could be observed. The integrity of the cell structure clearly declined. Fig. 5C shows the result of the TAX-F127 group, which displays similar results to the TAX-H<sub>2</sub>O group, consistent with the above-mentioned results. Significantly, in the TAX-CP group as shown in Fig. 5D, the largest area of cell necrosis was observed. Integrated cell structures could almost not be found and the distribution of cells was greatly loosened compared with the control groups, further demonstrating a superior anti-cancer effect of the TAX-CP system.

## 4. Conclusion

In summary, the preliminary application of a self-healing CP hydrogel as a drug carrier was studied using Taxol as a drug model. Through *in vitro* and *in vivo* experiments, numerous advantages of this CP hydrogel were demonstrated, such as rapid self-healing after injection, precise delivery of the drug to the desired position, stable control of the release of the encapsulated drug, and minimal toxicity or side effect of the naked drug. This self-healing CP hydrogel has proven to be a better candidate in intra-tumor drug therapy than the traditional injectable but non-self-healable hydrogel, suggesting that the drug carrier can work as the partner of the drug to improve the therapy efficiency. We believe that the CP hydrogel

has great potential not only in tumor chemotherapy but also in other biomedical research and has further clinical applications as a promising drug delivery system for various drugs.

## Acknowledgements

The authors thank the National Natural Science Foundation of China (81671757, 21534006, 21574008, 81671829) for its financial support.

## Notes and references

- K. Kataoka, A. Harada and Y. Nagasaki, *Adv. Drug Delivery Rev.*, 2001, **47**, 113.
- J. Panyam and V. Labhasetwar, *Adv. Drug Delivery Rev.*, 2003, **55**, 329.
- Y. Qiu and K. Park, *Adv. Drug Delivery Rev.*, 2001, **53**, 321.
- D. E. Owens 3rd and N. A. Peppas, *Int. J. Pharm.*, 2006, **307**, 93.
- M. J. Roberts, M. D. Bentley and J. M. Harris, *Adv. Drug Delivery Rev.*, 2012, **64**, 116.
- X. Gao, Y. Cui, R. M. Levenson, L. W. Chung and S. Nie, *Nat. Biotechnol.*, 2004, **22**, 969.
- D. Peer, J. M. Karp, S. Hong, O. C. Farokhzad, R. Margalit and R. Langer, *Nat. Nanotechnol.*, 2007, **2**, 751.
- M. J. Chen, Z. Z. Shao and X. Chen, *J. Biomed. Mater. Res., Part A*, 2012, **100**, 203.
- Y. Tian, X. Jiang, X. Chen, Z. Shao and W. Yang, *Adv. Mater.*, 2014, **26**, 7393.
- Z. Tu, M. Volk, K. Shah, K. Clerkin and J. F. Liang, *Peptides*, 2009, **30**, 1523.
- L. Chen, Z. G. Tu, N. Voloshchuk and J. F. Liang, *J. Pharm. Sci.*, 2012, **101**, 1508.
- C. C. Chuang and C. W. Chang, *ACS Appl. Mater. Interfaces*, 2015, **7**, 7724.
- R. Y. Huang, P. H. Chiang, W. C. Hsiao, C. C. Chuang and C. W. Chang, *Langmuir*, 2015, **31**, 6523.
- J. Fang, H. Nakamura and H. Maeda, *Adv. Drug Delivery Rev.*, 2011, **63**, 136.
- V. Torchilin, *Adv. Drug Delivery Rev.*, 2011, **63**, 131.
- V. P. Torchilin, *Pharm. Res.*, 2007, **24**, 1.
- H. Y. Lee, Z. Li, K. Chen, A. R. Hsu, C. Xu, J. Xie, S. Sun and X. Chen, *J. Nucl. Med.*, 2008, **49**, 1371.
- W. J. Mulder, R. Koole, R. J. Brandwijk, G. Storm, P. T. Chin, G. J. Strijkers, C. de Mello Donegá, K. Nicolay and A. W. Griffioen, *Nano Lett.*, 2006, **6**, 1.
- R. M. Schiffelers, A. Ansari, J. Xu, Q. Zhou, Q. Tang, G. Storm, G. Molema, P. Y. Lu, P. V. Scaria and M. C. Woodle, *Nucleic Acids Res.*, 2004, **32**, e149.
- R. K. Jain, *Sci. Am.*, 1994, **271**, 58.
- Q. Feng, K. Wei, S. Lin, Z. Xu, Y. Sun, P. Shi, G. Li and L. Bian, *Biomaterials*, 2016, **101**, 217.
- S. V. Wegner, F. C. Schenk, S. Witzel, F. Bialas and J. P. Spatz, *Macromolecules*, 2016, **49**, 4229.
- Y. Guan and Y. Zhang, *Chem. Soc. Rev.*, 2013, **42**, 8106.
- M. Guvendiren, H. D. Lu and J. A. Burdick, *Soft Matter*, 2012, **8**, 260.
- D. S. Benoit, C. R. Nuttelman, S. D. Collins and K. S. Anseth, *Biomaterials*, 2006, **27**, 6102.
- T. R. Hoare and D. S. Kohane, *Polymer*, 2008, **49**, 1993.
- N. Bhattarai, J. Gunn and M. Zhang, *Adv. Drug Delivery Rev.*, 2010, **62**, 83.
- N. Bhattarai, H. R. Ramay, J. Gunn, F. A. Matsen and M. Zhang, *J. Controlled Release*, 2005, **103**, 609.
- L. Yu and J. Ding, *Chem. Soc. Rev.*, 2008, **37**, 1473.
- H. D. Lu, D. E. Soranno, C. B. Rodell, I. L. Kim and J. A. Burdick, *Adv. Healthcare Mater.*, 2013, **2**, 1028.
- L. Ruan, H. Zhang, H. Luo, J. Liu, F. Tang, Y. K. Shi and X. Zhao, *Proc. Natl. Acad. Sci. U. S. A.*, 2009, **106**, 5105.
- C. T. Wong Po Foo, J. S. Lee, W. Mulyasmita, A. Parisi-Amon and S. C. Heilshorn, *Proc. Natl. Acad. Sci. U. S. A.*, 2009, **106**, 22067.
- Y. Zhang, L. Tao, S. Li and Y. Wei, *Biomacromolecules*, 2011, **12**, 2894.
- B. Yang, Y. Zhang, X. Zhang, L. Tao, S. Li and Y. Wei, *Polym. Chem.*, 2012, **3**, 3235.
- C. Zhu, J. Zhao, K. Kempe, P. Wilson, J. Wang, T. Velkov, J. Li, T. P. Davis, M. R. Whittaker and D. M. Haddleton, *Macromol. Biosci.*, 2016, DOI: 10.1002/mabi.201600320.
- Y. Li, Y. Zhang, F. Shi, L. Tao, Y. Wei and X. Wang, *Colloids Surf., B*, 2017, **149**, 168.
- J. Sanceau, M.-F. Poupon, O. Delattre, X. Sastre-Garau and J. Wietzerbin, *Oncogene*, 2002, **21**, 7700.